the first MTT National Lecturer in 1967. He was named an Outstanding Educator of America in 1973, and in 1974 he received a Sigma Xi Citation for Distinguished Research. He has received prizes for two of his papers: the IEEE Microwave Prize in 1967 and the Institution Premium, the highest award of the British IEE, in 1964. He was a National Chairman of the IEEE MTT Society, a member of the IEEE Publication Board, and General Chairman of three symposia. In 1977 he was elected an Honorary Life Member of the IEEE MTT Society. He is a past Chairman of Commission 1 (now A) and a member of Commission 6 (now B) of the International Union of Radio Science (URSI), and a former Chairman of a National Academy of Sciences Advisory Panel to the National Bureau of Standards.

Guidance and Leakage Properties of a Class of Open Dielectric Waveguides: Part II—New Physical Effects

ARTHUR A. OLINER, FELLOW, IEEE, SONG-TSUEN PENG, MEMBER, IEEE, TING-IH HSU, STUDENT MEMBER, IEEE, AND ALBERTO SANCHEZ

Invited Paper

Abstract—**A class of open dielectric waveguides is discussed which is of direct importance to the areas of integrated optics and millimeter-wave integrated circuits. An accurate analysis of the properties of these waveguides reveals that interesting new physical phenomena, such as leakage and sharp cancellation or resonance effects, may occur under appropriate circumstances. The resulting leaky modes form a new class of such modes since the leakage, in the form of an exiting surface wave, has a polarization opposite to that which dominates in the bound portion of the leaky mode. These new effects are caused by TE–TM mode coupling, which was neglected in earlier approximate treatments. Part II describes the new physical effects and includes numerical results on various waveguiding structures to illustrate the new effects quantitatively.**

I. Introduction

IN THIS PART, we first describe and discuss certain *new physical effects* that follow from taking into account the *coupling between TE and TM modes* that occurs at the sides of the open dielectric waveguides. Since such coupling is ignored completely in the customary approximate treatments, those treatments miss these physical effects entirely. Later in the paper various *numerical results* are presented for typical waveguiding structures which illustrate these new physical effects quantitatively, as well as indicating for which physical properties the approximate theories are satisfactory and for which they are not.

Manuscript received March 24, 1981; revised May 18, 1981. This work was supported by the Joint Services Electronics Program under Contract F49620-80-C-0077.

The authors are with the Department of Electrical Engineering and Computer Science, and the Microwave Research Institute, Polytechnic Institute of New York, Brooklyn, NY 11201.

Part I of this paper presents in detail the general mode-matching procedure which results in an accurate analysis of the propagation behavior of these open dielectric waveguides. In that treatment, the approach and the point of view are developed in detail; we will require them in our physical discussions below, and we briefly review them in the context of our summary in Section II of the "effective dielectric constant" approximation. Following the summary of that approximate method, we show in Section II-B the physical consequences of improving that approximation by including the TE–TM mode coupling at the sides of the open dielectric waveguide. Most importantly, we thereby obtain the new physical effects to be described, but we also show how the hybrid nature of these guided modes is altered. The *mathematical* consequences of accounting for the TE–TM coupling, with the implied inclusion of higher modes, are examined in detail in Part I.

The new physical effects to which we refer are the presence of *leakage* and the appearance of sharp *resonance*, or cancellation, *effects*. As mentioned earlier, the customary approximate theories neglected the TE–TM coupling and thus never predicted these physical effects. The effects themselves are discussed in Section III. We present, in Sections III-B and -C, physical explanations for the leakage mechanism and the resonance effect. The leakage occurs in the form of a surface wave which emerges from the guiding structure at some angle to it. The exit angle of the leaking surface wave is discussed in Section III-E.

The leakage to which we refer changes the guided mode

0018-9480/81/0900-0855$00.75 ©1981 IEEE

from being purely bound to a *leaky mode*. It is not generally known that leaky modes can exist on a large class of these open dielectric waveguides. In fact, as we show, some treatments which include the higher modes, and therefore the TE–TM coupling, have not recognized that leaky modes are present under appropriate conditions. These leaky modes also constitute *a new class* of leaky modes, in that the leakage portion of the leaky mode has a *polarization opposite* to that which dominates in the bound portion of the leaky mode. For example, if the guided mode is TM-like, meaning that the electric field of the mode is predominantly *vertically* polarized, the leaking surface wave portion will be a TE surface wave, with its electric field *horizontally* polarized. This interesting feature makes these leaky modes different from the usual types of leaky mode.

It is important for two reasons to know whether or not leakage is present. Since these dielectric waveguides are usually intended for use in an *integrated-circuit fashion*, unwanted leakage can cause crosstalk between neighboring components and thus deteriorate the performance of the circuit. On the other hand, novel components can be designed which make deliberate use of the leakage present. An example of such a component for integrated optics is a novel leaky-wave directional coupler [1], which can also serve as a mode stripper.

The class of open dielectric waveguides treated in this two-part paper comprises many different types of waveguiding structure, some of which have been illustrated in Fig. 1 of Part I, and others of which are shown in Figs. 3 and 4 below. The TE–TM coupling produced by the sides of the waveguides occurs in all of these open waveguide structures, with the result that all of them support hybrid modes possessing all six field components. However, not all these waveguides can support modes which leak; on some of these waveguides, all the modes are always purely bound, despite the TE–TM mode coupling. This statement applies, of course, only when the waveguide is uniform longitudinally and above cutoff (when the waveguide cross section is tapered, or when the structure is periodically loaded in an appropriate manner, leakage will result in customary fashion). Section III-A describes which types of waveguide can leak and which will never leak, and presents the reason why, together with illustrative examples.

On those waveguides which can leak, some modes will leak and some will not. In addition, of those modes which leak, one can change the geometry to avoid the leakage or, alternatively, alter the geometry to produce or enhance the leakage. A detailed prescription as to when leakage will or will not occur is contained in Section III-D. In general, however, the dominant guided mode on these waveguides will not leak, but the lowest mode of opposite polarization usually will.

Numerical examples which illustrate these new physical effects are presented in Section IV. The waveguides selected for these numerical calculations are the rib waveguide for integrated optics, and the dielectric ridge guide and the inverted strip guide for millimeter-wave integrated circuits. The complex propagation characteristics of these waveguides are obtained on use of the accurate mode-matching procedure described in detail in Part I; 15 modes of each type (TE and TM) are employed in the transverse resonance evaluations.

In Section II-A, comparisons are made between the values of β, the real part of the propagation wavenumber, obtained by using the approximate "effective dielectric constant" method and those computed via the accurate mode-matching method. It is shown that for most cases the approximate method yields results for β which are sufficiently accurate, but that sometimes noticeable differences occur. This approximate method cannot be used at all for determining the values of α (the leakage rate), however, because it neglects entirely the TE–TM coupling which gives rise to the leakage.

The new physical effects of leakage and resonance discussed in Section III are illustrated numerically in Section IV-B, where the values presented are calculated using the mode-matching procedure. The examples show that, depending on the type of waveguide and on the specific geometrical parameters, leakage may occur for any value of strip width or only for narrow strip widths. In addition, the rate of leakage may be large or small, and the exit angle of the leaking surface wave may also be large or small. Examples are presented which illustrate extremes as well as typical behavior.

Lastly, in Section IV-C, we include *experimental results* which demonstrate clearly that the variation of leakage with strip width obtained from measurements agrees very closely with theoretical predictions.

II. Review of Approximations

We first summarize some of the main features of the approach and point of view so that the physical explanations in Section III will be clear. Under Section II-A, we also summarize, for two reasons, the main features of the "effective dielectric constant" approximate procedure. The first reason is that we recommend that the procedure be used when approximate values, suitable for engineering applications, are required of only the real part, β, of the guided-mode propagation wavenumber. The other reason is that it is important to know the limitations of this popular approximate method, and what physical consequences follow from taking into account what is neglected in this approximation. The most important neglected feature is that of TE–TM coupling at the sides of the dielectric waveguide; the nature of this coupling, and its consequences, are discussed under Section II-B.

A. The "Effective Dielectric Constant" Approximation

The "effective dielectric constant" (EDC) approximation is a very simple and practical method for obtaining reasonably accurate values of β, the real part of the propagation wavenumber, of most open dielectric waveguides. The differences between values of β determined by this method and those calculated by an accurate mode-matching procedure are discussed in Section IV-A for several waveguiding structures.

The EDC method is actually quite an old one, being essentially the first step in a systematic transverse reso-

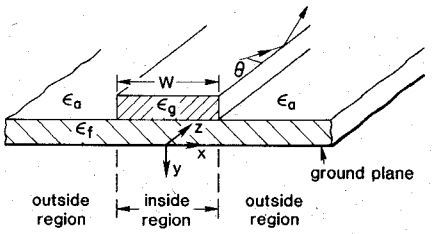

Fig. 1. A dielectric strip waveguide for millimeter-wave integrated circuits selected as a typical example. Shown on the figure is the division into constituent inside and outside regions, and one bounce of a constituent surface wave, at angle θ, as part of the guiding mechanism.

nance procedure. About a decade ago, it had already been applied to open dielectric guiding structures in millimeter waves [2], and even surface acoustic waves [3], [4]. More recently, it has been applied successfully to various dielectric waveguides for integrated optics and millimeter waves [5]–[7], and even to thin-film semiconductor lasers [8]. A somewhat similar approximate procedure, dubbed the "effective refractive index" method, was applied to dielectric strip waveguide structures for integrated optics when the refractive index of the strip is less than that of the film [9] or greater than that of the film [10]. It is an extension of the simple Marcatili approach [11], involving a patchwork procedure. In applying the EDC method it is of course unimportant whether the dielectric constant ϵ or the refractive index $n(=\sqrt{\epsilon})$ is employed; it is the procedure itself which is important.

In the EDC procedure, one follows the simple basic approach common not only to the approximate methods but also to the accurate mode-matching procedure. That approach is illustrated in Fig. 1 with respect to a dielectric strip waveguide for millimeter waves; the waveguide is a variant of the so-called "insular guide" [12], and consists of a dielectric strip placed on a wide dielectric film on a conducting ground plane.

The first step is to divide the cross section into *two constituent regions*, an "inside" region and "outside" regions, the inside and outside regions corresponding respectively to $|x|<W/2$ and $|x|>W/2$. Thus the inside region contains the guiding strip of dielectric constant ϵ_g and width W placed on the dielectric film on the ground plane, whereas the outside regions consist only of the dielectric film of dielectric constant ϵ_f located on the ground plane.

Within the inside (or central) region, comprised of the strip on the film on the ground plane, we assume that a surface wave can be supported. The customary viewpoint with respect to the guiding mechanism for a wave in the longitudinal (z) direction is that a pair of these surface waves will then bounce back and forth horizontally in this central region at an angle between the sides of the strip, undergoing total internal reflection at each bounce. One such bounce, at angle θ, is shown in Fig. 1.

In the EDC procedure, each of the two constituent regions is viewed as a slice out of, or a portion of, a planar waveguide of infinite width. Its guidance behavior is thus considered to be identical to that for a planar guide of infinite width. Each constituent region (treated as if it were infinitely wide) is then subjected to a (simple) transverse

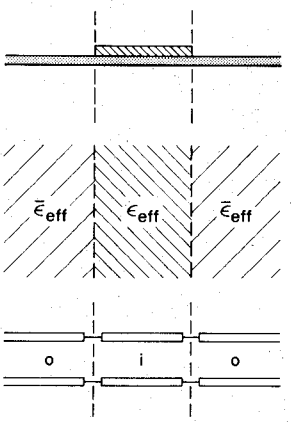

Fig. 2. A pictorial summary of the "effective dielectric constant" (EDC) approximate method. The constituent inside (i) and outside (o) regions are expressed as equivalent uniform dielectric regions, shown in the middle of the figure, characterized in terms of effective dielectric constants; the transverse resonance is thus given by the simple equivalent network shown at the bottom.

resonance analysis, taken in the *vertical* (y) direction, to determine the dispersion properties of the propagating surface wave modes in the respective regions. These dispersion properties are expressed in terms of the effective refractive index n_{eff} or the effective dielectric constant $\epsilon_{\text{eff}}(=n_{\text{eff}}^2)$ for each of the regions. Thus, each of the constituent (inside and outside) regions of Fig. 1 can be viewed as an equivalent *uniform* dielectric region, and the complete structure can be regarded as three uniform regions contiguous to one another, as seen in Fig. 2, which presents a pictorial summary of the EDC method.

In this approach, the *geometrical discontinuities* corresponding to the sides of the strip have been avoided altogether. If we were to set up a transverse equivalent network to describe such a junction of equivalent uniform dielectric regions, we would obtain the direct connection of transmission lines shown at the bottom of Fig. 2. If the geometrical discontinuities were not neglected, then additional lumped elements would have to be placed at the junctions between the transmission lines. Furthermore, only a single transmission line need be used for each constituent region because it has been assumed all along that *only one* surface wave is present in each region.

To complete the derivation, one next performs a transverse resonance in the *horizontal* (x) direction, assuming that each constituent region is represented by an effective uniform dielectric medium; finally, one relates the various transverse wavenumbers to the desired longitudinal one by the customary sum-of-squares relations.

The mathematical steps corresponding to the descriptive remarks made here are presented in Section II of Part I.

Two basic assumptions have been made in this analysis (and also in other approximate analyses):

1) only a single surface wave is present in each of the constituent regions; and
2) the geometrical discontinuities corresponding to the sides of the step are neglected altogether.

Under most circumstances, at least two surface waves, one TE and one TM, are capable of being supported

simultaneously. However, these two surface waves are independent of each other in uniform regions, and they couple to each other only at geometrical discontinuities. Thus, if the assumptions above were *not* imposed, then both the TE and the TM surface waves would need to be included in the analysis, and these surface waves would be coupled at the strip sides. In the next section we consider some of the physical consequences of such coupling.

B. TE–TM Coupling

As we saw in the section above, the cross section of the dielectric waveguide of Fig. 1 is considered to consist of two constituent regions, the inner strip region and the outer portions. We also noted that approximate theoretical analyses for the propagation characteristics of strip waveguides assume the presence of only one mode type, TE or TM, in each of the constituent regions comprising the cross section of the strip waveguide. When the field behavior at the strip sides is viewed more carefully, however, it is easy to see that a TE or TM surface wave incident on a strip side at an angle produces not only a reflected and a transmitted wave of its own type, but also excites a reflected and a transmitted wave of the other type (polarization). Because of its geometrical discontinuity, the strip side also excites a continuous spectrum, if the region is completely open, or all the higher discrete modes, if the structure is bounded far above by a conducting plate, as is done in Part I to discretize the modal spectrum and make it more amenable to a mode-matching analysis. In any case, one can show by examining the wavenumbers that all components of this continuous spectrum, or its discrete equivalent, are purely nonradiative here.

To see why such cross-coupling between surface wave modes must occur, consider first a TE surface wave propagating along an infinitely-wide planar structure identical to that in the strip region. If the wave is propagating in the z direction, it has only the following field components: H_y, H_z, and E_x. If, however, the wave travels at a small angle with respect to the z direction, additional small components H_x and E_z arise. Similarly, a TM surface wave traveling at a small angle in that configuration will possess not only components E_y, E_z, and H_x, but also small amounts of E_x and H_z. When such a TE wave bounces back and forth in the actual strip region, it hits the strip sides at a small angle with respect to the z direction; the small H_x and E_z field components then excite a TM surface wave at the strip sides. Similarly, the small E_x and H_z components of an incident TM surface wave will excite a TE surface wave there. Thus TE–TM surface-wave mode coupling *necessarily* occurs at these strip sides.

It is shown in Section III that it is just this coupling that gives rise to the new physical effects of leakage and resonance under appropriate circumstances. We add here only certain remarks on how the *hybrid nature* of the modes guided along the strip structure of Fig. 1 (and correspondingly for all open dielectric waveguides in this class) become affected by this TE–TM coupling.

In the effective dielectric constant procedure, and in other one-mode approximate procedures, the guided modes propagating in the longitudinal (z) direction are found to be hybrid in that direction. The guided modes are hybrid because the constituent TE *or* TM modes bounce against the sides of the waveguide at an angle to the longitudinal direction, thereby producing components of both the electric and magnetic fields in the longitudinal (z) direction. However, those hybrid modes possess only 5 field components, lacking a vertical (y) electric field component if a TE mode bounces against the sides, or a vertical magnetic field component if a TM mode does. Such hybrid modes can therefore be characterized as LSE or LSM modes, respectively, or as H-type or E-type, respectively, with respect to the y direction, depending on one's preference in notation.

When the TE–TM coupling at the sides of the dielectric waveguide is taken into account, the hybrid modes now become more complex, possessing 6 field components instead of 5. Although these modes can no longer be characterized according to whether they possess, in the vertical direction, only a magnetic field component or only an electric field component, the amount of the other vertical field component is usually small because the TE–TM coupling itself is usually small. It becomes convenient then to characterize these hybrid modes as *TE-like* or *TM-like*, depending on which surface wave that bounces back and forth between the sides has the predominant field energy.

For example, let us assume that the waveguide of Fig. 1 is excited by an incident wave possessing a vertical magnetic field. A wave with that field polarization will set up a pair of TE surface waves in the central strip region which bounce back and forth between the strip sides. At each bounce, a small amount of mode conversion into a TM surface wave takes place; this TM surface wave then also bounces back and forth, producing TE mode conversion at each bounce, continuing the process. The resulting guided mode in the longitudinal (z) direction is then a hybrid mode containing a combination of the TE and the TM surface waves, but the mode energy resides predominantly in the TE portion. The guided mode is therefore a TE-like hybrid mode.

It should also be observed that the incident (exciting) field will not in general exactly match the field of the resulting TE-like hybrid mode. This mismatch will excite a small amount of energy in a TM-like hybrid guided mode, which is usually also above cutoff at the same time. Thus the incident TE polarization will actually set up two linearly-independent guided modes, one which is TE-like and one which is TM-like, with most of the power being in the TE-like mode. The TE-like mode will possess a large vertical magnetic field component and a small vertical electric field component; the situation is reversed for the TM-like mode. The proportion of energy in these two guided modes will depend on the form of the exciting field.

III. The New Physical Effects

The new physical effects which result from TE–TM coupling at the sides of the guiding structure are *leakage*, which changes a guided mode into a leaky mode, and a *resonance* or *cancellation* effect, which prevents leakage at

specific parameter values and which may also influence the value of β of the guided mode.

This section first considers the classes of open dielectric waveguide which are of use (or potential use) in integrated optics or millimeter-wave integrated circuits, and discusses why some of these waveguides can leak and why some will never leak. Next, it presents physical explanations for the leakage effect and for the resonance effect. For those waveguides which can leak, a discussion is presented next on criteria as to which modes leak and which do not, making use of the dispersion curves for the planar surface waves which are present in the inside and outside constituent regions. The section then ends with a description of how to determine simply the exit angle of the leaking surface wave.

A. Which Waveguides Leak and Which Do Not

Open dielectric waveguides have become increasingly important within the past few years, particularly in connection with the areas of integrated optics and millimeter-wave integrated circuits. The major types of waveguide being investigated in these two areas are presented in Figs. 3 and 4. As seen, these waveguides are associated with either a substrate or a ground plane; we are not concerned here with fiber waveguides of circular cross section.

It is not generally known that most modes on most of these waveguides can be *leaky*, instead of being purely bound, as is customarily assumed. As mentioned above, the widely-accepted tacit assumption that these modes are completely bound is based largely on published theoretical propagation characteristics, which are obtained from approximate analyses that neglect those features which lead to the leakage effects.

In the waveguides shown in Figs. 3 and 4, some structure is present in each case which is limited in extent in the horizontal direction in order to confine the fields laterally as well as vertically. These waveguides may be broadly divided into two classes:

1) those which are essentially modifications of dielectric rods of rectangular cross section; and
2) those which are formed by a dielectric strip that perturbs a planar dielectric waveguide.

Waveguides (a) and (b) of Fig. 3 and the rectangular image line of Fig. 4 fall into class 1, and the remaining waveguides are seen to belong to class 2. These two classes function differently physically, and, as will be seen, modes on waveguides in class 1 are always purely bound, whereas most modes on waveguides in class 2 can be leaky. The distinction between these two classes is therefore important with respect to the leakage question.

The two waveguides in class 1 which are shown in Fig. 3 consist of a strip either deposited on top of a substrate or diffused into it. In the latter case, the waveguide boundaries may not be sharp but the mode guidance behavior is unchanged in a qualitative sense. In the absence of the strip, no wave can be sustained because a normal dielectric half-space cannot support a mode. The strip therefore is itself the guiding vehicle, and the substrate serves only to modify the modal behavior and field distribution. The guidance behavior is thus that of a dielectric rod (or strip) modified by the presence of the substrate. For the dielectric image line of Fig. 4, it is clear that the structure is that of a rectangular dielectric rod and that the guiding action would vanish in its absence.

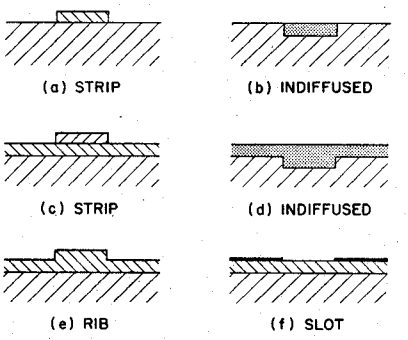

Fig. 3. Examples of open dielectric waveguides for integrated optics, where each waveguide is placed on a dielectric substrate. Waveguides (a) and (b) fall into the class for which no leakage is possible; the rest are members of the class for which some modes may leak.

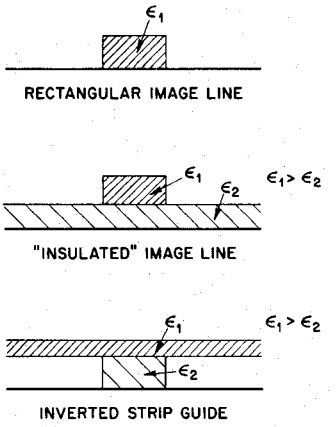

Fig. 4. Examples of open dielectric waveguides for millimeter-wave integrated circuits, where each waveguide is placed on a metal ground plane. Some modes on the "insulated" image line and the inverted strip guide may leak, whereas all modes on the rectangular image line are purely bound.

In those waveguides which fall into class 2, a wide planar dielectric layer is present. Thus, if the strip were not present, wave guidance would still occur because the dielectric film or layer provides a planar waveguide. The function of the strip is therefore to confine laterally the already-existing planar (wide) surface wave.

The advantage of such an arrangement for the waveguide of Fig. 3(c) was first pointed out by Furuta *et al.* [9], who observed that the modal properties of a strip on a substrate would be influenced strongly by the precise geometry of the strip, and that at optical wavelengths it is difficult to maintain geometrical uniformity on the strip. They proposed the geometry of Fig. 3(c), where the refractive index of the strip would be *less* than that of the film. Then, the strip would serve to pull in the field laterally but, since most of the field would still be concentrated in the film, the precise dimensions of the strip would be of lesser importance. A similar argument was presented by Itoh [6] for the inverted strip guide of Fig. 4.

As we discussed earlier, the customary explanation for the guidance mechanism in all of the waveguides in Figs. 3 and 4 proceeds by first dividing the waveguide cross section into two constituent regions—an inside region corresponding to the strip portion, and the outside regions, where the strip is absent. Within the inside region, the strip plus substrate or ground plane (in class 1) or the strip plus film plus substrate or ground plane (in class 2) supports one or more surface waves. If the excitation of the waveguide possesses a vertical electric field polarization, for example, the surface wave is of the TM type. This surface wave will then bounce back and forth horizontally in this central region at an angle between the sides of the strip, undergoing total internal reflection at each bounce.

In order to guarantee such total reflection, the inside, or central, guiding region must have an effective refractive index higher than that of the outside regions. There are, of course, many ways to achieve this arrangement; the most common ones are shown here. The waveguide in Fig. 3(e), known as a rib waveguide, is a special case of the strip waveguide in Fig. 3(c), where the strip and film materials are the same. These rib waveguides have been studied by and are being used by people at the Bell Laboratories [13], [14]. The structure in Fig. 3(d) is an indiffused or ion-implanted version [15], [16] of the rib waveguide, but where the guide boundaries are not as clearly defined and where the refractive index may vary within the guiding region. It has the advantage, however, of a smooth top surface. The slot waveguide in Fig. 3(f) consists of metal coatings on the outside regions, whereas the inside region is left unmodified. At optical frequencies, a metallic layer does not behave like a short circuit, but like an overdense plasma; that is, the dielectric constant of the metal is negative real. Thus, the metal coatings lower the effective refractive index of the outside regions, leaving the unmodified central region with a higher relative index. This type of waveguide was first proposed [17] in analogy to slot waveguides for surface acoustic waves, and later independently by others [18]. It has also been studied in some detail [19]–[21]. The geometry lends itself particularly readily to modulator applications, since a dc or RF field can be placed directly between the metal coatings. On the other hand, all of these guiding structures have been built and tested in the context of directional couplers, modulators, or switches.

The "insulated" image line and the inverted strip guide for millimeter-wave integrated circuits, shown in Fig. 4, were proposed as structures to reduce the metal loss at higher frequencies due to the metal ground plane in the dielectric image line. Because the dielectric constant ϵ_2 is lower than ϵ_1, the structure can be designed so that the fields decay exponentially in the vertical direction in the region of ϵ_2, and the currents in the ground plane become greatly reduced.

It was stated in that when these waveguides leak the leakage occurs in the form of a surface wave that travels away from the waveguide at some angle. Each of the waveguides in class 2 has dielectric wings, that is, a wide dielectric planar layer that can guide a surface wave in the absence of the central strip which concentrates the field laterally. The waveguides in class 2 therefore possess the geometric configuration that could sustain a leaking surface wave.

The waveguides in class 1, on the other hand, do not have the dielectric outer structure that could support a leaking surface wave. The guided modes for those waveguides are therefore purely bound. It is necessary, of course, to determine whether or not leakage is possible from such waveguides in the form of a constituent of the continuous spectrum that is excited at the strip sides. An examination of the relative wavenumber values, however, clearly rules out any such possibility.

We may therefore assert that all modes on waveguides belonging to class 1 are purely bound, but that it is possible for some modes on waveguides belonging to class 2 to leak in the form of a surface wave which exits from the waveguide at some angle and is supported by the waveguide's dielectric wings.

B. Physical Explanation of the Leakage Effect

As a typical waveguide belonging to class 2, let us consider the millimeter-wave dielectric strip waveguide appearing in Fig. 1, and discussed earlier in Section II-A, in connection with the approximate EDC method. The waveguide is a form of the "insulated" image line shown in Fig. 4.

As described in Section II-A, we divide the cross section into inside and outside constituent regions, designated, respectively, by *i* and *o*. If the exciting field produces a TE mode primarily in the waveguide, then, in the EDC analysis, the guiding process involves a TE surface wave bouncing back and forth in the inside (strip) region at an angle to the strip sides, undergoing total reflection at each bounce. In the transverse equivalent network in Fig. 2, the TE_i and TE_o transmission lines are above and below cutoff, respectively.

The layer thickness, however, is usually such that a TM surface wave can also be supported in each region. Then, as discussed in Section II-B, the TE and the TM surface waves become necessarily coupled to each other at the sides of the strip because of the geometrical discontinuities there. As a result, the simple EDC equivalent network shown in Fig. 2 becomes replaced by the transverse equivalent network appearing in Fig. 5, which takes into account the aforementioned TE–TM coupling.

Actually, the network in Fig. 5 is almost rigorous, neglecting only any higher mode interactions that may occur between the two strips sides if the strip width is sufficiently small. The boxes in the network represent the coupling between the TE and TM modes, and also the modal content of the continuous spectrum (or its discrete equivalent) excited by the strip sides. These boxes are purely reactive since the continuous spectrum is nonradiating under the conditions of mode guidance, as may be readily verified by an examination of the relative wavenumber values.

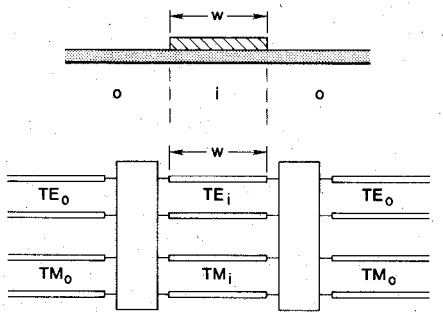

Fig. 5. Transverse equivalent network for an open dielectric strip waveguide which takes into account the TE–TM mode coupling produced at the sides of the strip. The symbols *i* and *o* represent, respectively, the inside (strip plus layer) and outside (layer) constituent portions of the waveguide cross section.

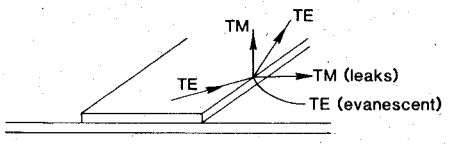

Fig. 6. Pictorial ray representation of the TE–TM mode-coupling process at one side of a dielectric strip waveguide. The coupling shown here produces leakage of a TM surface wave in the outside region when a TE surface wave is incident on the strip side from the inside region.

In the approximate EDC analysis discussed in Section II-A, the TE–TM coupling is neglected and only one transmission line, the TE one, say, is considered. Consistent with the total reflection viewpoint, the TE_i transmission line is above cutoff whereas the TE_o ones are below cutoff, and the guided wave is purely bound in this approximate analysis. Since the TM surface wave is the lowest surface wave (possessing the highest ϵ_{eff}) in this structure, it is shown in Section III-D below that, when the TE–TM mode coupling is included, and the complete network in Fig. 5 is used, the TM transmission lines can be *above* cutoff in *both* the inside and outside regions. If the TM_o transmission line in Fig. 5 is above cutoff, then leakage of energy from the TE_i surface wave into the TM_o surface wave will occur at each bounce at the strip sides, and a *leaky mode* will result. This situation is pictorially summarized in Fig. 6.

The leakage, when it occurs, is thus due to the coupling between the constituent TE and TM waves produced at the strip sides when these waves bounce back and forth in the strip region, as part of the guiding process. In Fig. 6 (as in Fig. 1), let us take the waveguide axial direction to be the z direction, and the horizontal direction in the cross section to be the x direction. Let us also choose the TE surface wave to be the one which the incident field excites primarily, so that leakage occurs in the TM surface wave outside, if it occurs at all. These considerations are consistent with the qualitative discussion above. The explicit condition for leakage is then

$$\left(k_x^{\text{TM}}\right)_{\text{out}}^2 > 0. \tag{1}$$

The quantity $(k_x^{\text{TM}})_{\text{out}}$ is the transverse wavenumber of the TM surface wave in the outside region, and relation (1) states that the outer TM transmission line in the transverse equivalent network in Fig. 5 is above cutoff (propagating).

The resonances of the transverse equivalent network in Fig. 5 then yield the wavenumbers of the hybrid modes guided by the waveguide in the axial direction. These wavenumbers are complex when leakage is present, and the value of α of a leaky mode is the measure of its leakage rate.

C. Physical Explanation of the Resonance Effect

Fig. 6 represents pictorially the results of TE–TM coupling at a strip side. As shown, a TE surface wave incident on the strip side mode converts in part into a TM surface wave outside and a TM surface wave inside. If the TM surface wave in the *outside* region is above cutoff, then, as discussed in Section III-B, the TE-like guided mode becomes leaky, and leakage of TM surface wave energy occurs.

We now consider the TM surface wave in the *inside* region. This mode-converted surface wave is almost always *above* cutoff, so that it also bounces back and forth between the strip sides as part of the guiding process.

One observes in the curves of the leakage rate α versus the strip width W, for certain geometrical parameter combinations, that very sharp and steep dips occur for specific values of W. A typical example is provided by Fig. 13. At these values of W the leakage appears to be cancelled, and the behavior is akin to a *resonance* effect. This effect is due to the mode-converted surface wave which is bouncing back and forth above cutoff in the *inside* region. From a simple calculation, we find from the curves that, to within 1 percent, the condition for the resonances is given by

$$\left(k_x^{\text{TM}}\right)_{\text{in}} W = 2m\pi, \qquad m = 1, 2, \cdots \tag{2}$$

if the mode-converted surface wave is TM, and correspondingly for TE. The quantity $(k_x^{\text{TM}})_{\text{in}}$ is of course the transverse wavenumber of the TM surface wave in the inside (strip) region.

The equivalent networks presented in Part I to describe in pictorial fashion the way in which the various transverse modes couple together at the sides of the strip can be recast in a form which sheds light on the resonance process. From the recast network it can be shown that the cancellation effect is not complete, but almost so. When only one TM mode and one TE mode is included in each region, complete cancellation occurs in accordance with condition (2), but the presence of higher modes softens the completeness of the cancellation. Nevertheless, it is seen from various accurate numerical calculations that the resonance dips are at least four orders of magnitude below the peaks in the attenuation plots; for engineering purposes it is therefore safe to regard the dips as equivalent to nulls even though they are rigorously not so. The proof of these statements will be presented elsewhere.

We have performed a similar analysis for a slot waveguide [20] for integrated optics, and the numerical results show that the resonance effect dramatically reduces not

only any leakage produced, but also the attenuation due to the presence of the metal.

D. Which Modes Leak and Which Do Not

Whether or not leakage will occur in a specific case can be assessed by looking at the *dispersion curves* for the *planar* surface waves in each of the *constituent* regions comprising the cross section of the dielectric waveguide. As an illustration of how to use these curves, let us here consider the simpler case of the ridge waveguide for millimeter waves, obtained by making the strip and the film of the same dielectric material in the dielectric strip waveguide of Fig. 1. The dispersion plots for the inside and outside constituent regions are then the same, differing only in the thickness of the dielectric layer.

The planar dispersion plots for the constituent regions of the dielectric ridge structure are shown in Fig. 7. The lowest surface wave mode is the TM_0, and the next one is the TE_1, as seen in Fig. 7. The vertical line t_1 corresponds to the (thicker) strip region, and the line t_2 to the outside (film) regions, as indicated in the inset in Fig. 7.

For *complete* guiding, all the surface waves bouncing back and forth inside the strip region at an angle to the strip sides must be propagating, and all the surface waves present outside must be evanescent. Suppose that the waveguide is excited with the electric field oriented in the horizontal (x) direction, so that the basic excitation is "TE," corresponding to point 1 shown in Fig. 7. As this TE wave bounces back and forth inside the strip region, it couples some TM energy at each reflection from the strip sides. The TE wave outside is always evanescent transversely, as required, but what can we determine about the TM wave outside? We must examine the relative n_{eff} values on the dispersion curves to see whether or not the TM_0 surface wave is evanescent. From Fig. 7 one sees that the value of n_{eff} for the TM_0 surface wave outside (at thickness t_2), identified as point 2, is *even larger* than the value of n_{eff} for the TE_1 surface wave *inside* (at thickness t_1), at point 1. The TM_0 surface wave outside is thus seen to be propagating rather than evanescent. Hence, the condition for complete guiding is *not* satisfied, and the hybrid TE-like mode is *leaky*, consistent with the picture in Fig. 6.

If the initial waveguide excitation were of the "TM" type, a corresponding inquiry would indicate that the resulting hybrid guided wave would be completely bound. Thus the guided TM-like modes on *this* waveguide corresponding to the excitation of the TM_0 surface wave in the inside region will *not* leak.

Depending on how close the dispersion curves in Fig. 7 are to each other, the TM_0 wave outside may or may not be evanescent, so that the resulting TE-like guided mode may or may not be leaky. For the case shown here, the mode will be leaky for *any* value of strip width W. For a different set of geometrical parameters, the guided mode may be leaky only for narrow strips but not for wide strips. We have developed a simple criterion for leakage, employing these planar dispersion curves, which permits a systematic method for predicting when leakage will occur, but it will be presented elsewhere [22]. However, we summarize later some of the main results deduced from this procedure.

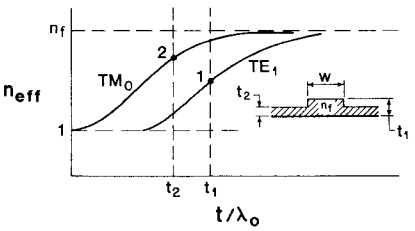

Fig. 7. Planar dispersion plots for the two lowest surface waves in each of the constituent regions comprising the cross section of the dielectric ridge waveguide shown in the inset. The vertical lines t_1 and t_2 correspond respectively to the inside and outside regions. The plots are used to determine which modes leak and which do not.

For any dielectric waveguide configuration, one must first determine which surface wave will be the dominant one in the inside constituent region. If it is a TM surface wave, as in the waveguide of Fig. 1, then we can make the set of statements given below; if the dominant surface wave is TE, then the conclusions are valid when TE and TM are interchanged.

We should also recall that each of the (hybrid) guided modes of a dielectric strip waveguide is based on a particular surface wave mode which is excited in the central strip region. For example, if the strip region is excited with the electric field polarized vertically, the surface wave in the strip region will be a TM surface wave, and the resulting set of guided modes will be TM-like. There may be more than one of these guided modes, depending on the strip *width*. If the strip *thickness* is sufficiently large, then more than one TM surface wave may be excited in the strip region; in that case one set of hybrid TM-like guided modes will exist for each of these surface waves. Now, assuming that the dominant constituent surface wave is TM, we may draw the following general conclusions.

a) TM-like (hybrid) guided modes of the dielectric strip waveguide which are based on the *lowest* TM constituent surface wave are always purely bound (never leaky).

b) TE-like or TM-like guided modes based on *higher order* TE or TM constituent surface waves are always leaky.

c) TE-like guided modes based on the *lowest* TE constituent surface wave may or may not be leaky, but usually are. If the TE and TM constituent surface-wave dispersion curves are not close to each other, the TE-like guided modes will be leaky for all values of strip width. If these dispersion curves lie very close to each other, the TE-like guided modes will be leaky only for narrow strip widths.

In determining which surface wave is the lowest one in the planar constituent regions, one must be careful because for some few structures the choice of which surface wave is dominant changes with dimensional parameter values. An example of such a changeable structure is the inverted strip guide (see Fig. 4) proposed by Itoh [6] for millimeter waves; that versatile waveguide can be designed so that it does not leak, or can leak a TE surface wave while guiding

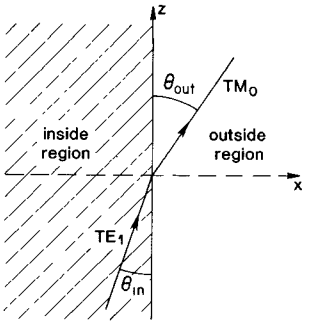

Fig. 8. Pictorial ray representation of the exit angle θ_{out} of the leaking surface wave. The region to the left corresponds to the inside region of the waveguide.

a TM-like hybrid mode, or can leak a TM surface wave while guiding a TE-like mode.

E. The Exit Angle of the Leaking Surface Wave

If the hybrid guided mode on the dielectric waveguide is leaky, the above-discussed dispersion curves for the constituent regions may be used to help determine the exit angle of the leaking surface wave. Suppose the TE-like hybrid guided mode on our dielectric ridge waveguide in Fig. 7 is leaky, and we wish to determine the *angle* which the leaking TM_0 surface wave makes with the longitudinal (z) axis of the waveguide. The situation is depicted in Fig. 8, where θ_{out} is the angle we seek. Suppose also that a solution for the real part β_z of the propagation wavenumber of the guided mode has been obtained, for example, by using the EDC method; such an approximate solution is sufficient for this purpose, and is easy to compute. Then, by inspection of Fig. 8, we see that

$$\cos\theta_{out} = \frac{\beta_z}{\left(k_s^{TM_0}\right)_{out}} = \frac{(n_{eff})_{guide}}{\left(n_{eff}^{TM_0}\right)_{out}} \tag{3}$$

where $(k_s^{TM_0})_{out}$ is the wavenumber of the TM_0 surface wave in the outside regions; upon division by the free-space wavenumber k_0 the ratio involving the n_{eff} values is obtained. The value $(n_{eff}^{TM_0})_{out}$ is found directly from the TM_0 dispersion curve in Fig. 7 at the abscissa value t_2/λ_0; it is in fact the value indicated as point 2.

The exit angle θ_{out} may be very small, say a few degrees, as occurs in some integrated optics waveguides, or it can be quite large, like 45°, as is found in certain structures for millimeter waves. To a good approximation, the n_{eff} value for the TE-like hybrid guided mode is bracketed as follows:

$$\left(n_{eff}^{TE}\right)_{out} < (n_{eff})_{guide} < \left(n_{eff}^{TE}\right)_{in}.$$

Therefore, the $(n_{eff}^{TM})_{out}$ may be only very slightly larger than the $(n_{eff})_{guide}$ or substantially larger than it, depending on circumstances. Again, the dispersion plots offer insight.

For narrow strip widths, the $(n_{eff})_{guide}$ lies closer to the $(n_{eff}^{TE})_{out}$ value. For this reason, the exit angle θ_{out} will be larger for narrow strip widths and will decrease if the strip width is made to increase.

It should also be noted that the exit angle θ_{out} may be either greater or smaller than the angle θ_{in} in Fig. 8, where θ_{in} is given by

$$\cos\theta_{in} = \frac{(n_{eff})_{guide}}{\left(n_{eff}^{TE_1}\right)_{in}}. \tag{4}$$

When the waveguide is leaky for all values of the strip width W, a situation that corresponds to that in Fig. 7, $\theta_{out} > \theta_{in}$. However, when the dispersion curves are arranged so that leakage occurs only for narrow widths W, we find that $\theta_{out} < \theta_{in}$ when leakage is present.

IV. Numerical Examples

The new propagation effects discussed under Section III are illustrated numerically in this section with the help of the accurate mode-matching procedure presented in detail in Part I. For most of the examples, 15 modes of each type (TM and TE) are employed in the transverse resonance evaluations. Curves are presented for both the real part β and the imaginary part α of the propagation wavenumber of the hybrid guided modes of a variety of dielectric strip waveguides, with examples chosen from integrated optics and millimeter-wave integrated circuits.

For the real part β of the hybrid guided modes, we remarked in Section II-A that for most cases the approximate "effective dielectric constant" (EDC) method yields results that are sufficiently accurate for engineering purposes. We present in Section IV-A calculations of β for four different structures, showing that the EDC method is indeed very good in most instances, but that in others one must be careful. Section IV-B is concerned with the leakage and resonance effects, involving the attenuation constant α of the hybrid guided modes. Examples are presented for three different types of dielectric waveguide, illustrating a variety of features. Lastly, in Section IV-C, we present the results of an experiment, conducted recently in Japan, that demonstrates that the variation of leakage with strip width indeed follows the theoretical predictions very closely.

A. The Accuracy of Values of β Calculated via the EDC Method

Highly accurate values for β, the real part of the propagation wavenumber of the hybrid guided modes, can of course be obtained using the mode-matching procedure, described in detail in Part I. Since that procedure is quite involved, it is important to know if values which are sufficiently accurate for practical engineering purposes can be computed by means of a relatively-simple approximate procedure. The best such simple procedure is the "effective dielectric constant," or EDC, method, described in Section II-A.

We present now comparative calculations of β for four specific waveguides. The values of β found by means of the accurate mode-matching procedure discussed in Part I are represented by solid lines, while those obtained via the EDC method are indicated by dashed lines. For all cases, 15 TE and 15 TM modes were employed in the mode-

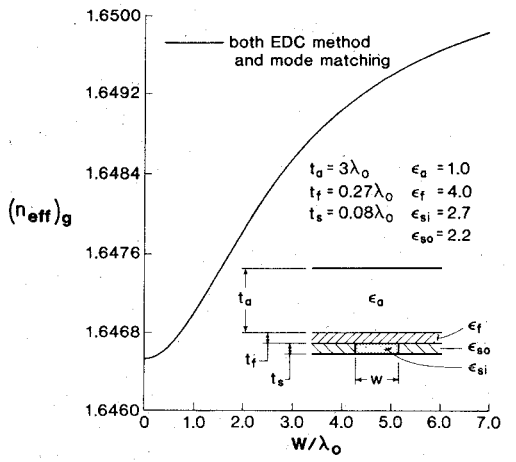

Fig. 9. Dispersion curve, in the form of $(n_{eff})_g$ versus W/λ_0, for the lowest TE-like hybrid guided mode of the inverted strip guide shown in the inset. (Dimension t_a in the inset is not drawn to scale.) For this structure, "TE" excitation results in a leaking TM surface wave. In this plot, the EDC and the accurate mode-matching calculations are indistinguishable from each other.

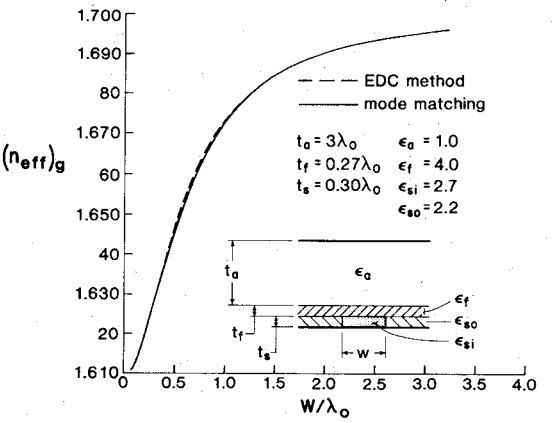

Fig. 10. Dispersion curve for the lowest TM-like guided mode of the inverted strip guide shown in the inset. (Dimension t_a in the inset is not drawn to scale.) This structure differs from that in Fig. 9 only in the value of t_s, but here a TE surface wave leaks. In this case, the EDC results differ very slightly from the accurate mode-matching values.

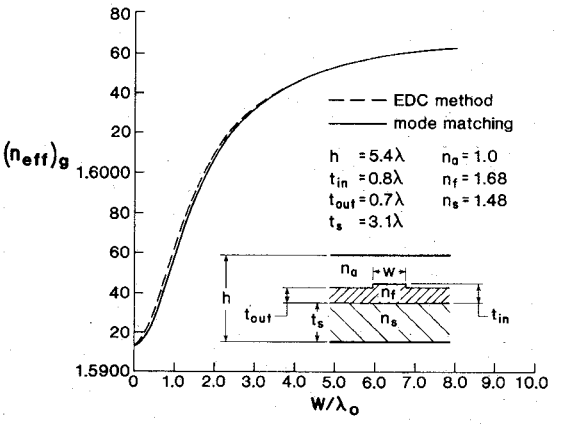

Fig. 11. Dispersion curve for the lowest TM-like guided mode on the rib waveguide for integrated optics shown in the inset. (Dimensions h and t_s are not drawn to scale.) Here, the EDC results are only slightly higher than the accurate mode-matching results.

matching procedure to insure accuracy; the EDC method, which involves only one surface wave mode in each transverse region, is less accurate but far simpler to use. It is seen below that in almost all cases the EDC results are of sufficient accuracy; sometimes they are indistinguishable on the curves from the highly accurate values, but at other times the differences between the accurate and approximate values are quite noticeable. One must therefore be cautious and not assume indiscriminately that the EDC results are always sufficiently accurate.

The first of the four waveguides is an inverted strip guide, with a relatively thick upper layer, as shown in the inset on Fig. 9. The geometry is so chosen that when the guided modes are TE-like, a TM surface wave leaks for all values of strip width. Right now we are concerned only with the values of β, however. Fig. 9 presents a dispersion curve of $(n_{eff})_g (= \beta_g / k_0)$, where the subscript g signifies the hybrid TE-like guided mode, as a function of W/λ_0, where W is the strip width, for the lowest TE-like guided mode. It is seen that for this case the EDC values are quite indistinguishable on the curve from the accurate mode-matching results.

The second case also involves an inverted strip guide, but with the geometry so arranged that when TM-like guided modes are present a TE surface wave leaks for any value of strip width. This polarization reversal was achieved by changing only the value of t_s. The values of $(n_{eff})_g$ versus W/λ_0 are shown in Fig. 10, and the geometry is indicated in the inset. For this case, the EDC and the accurate values are very close to each other, overlapping for small W/λ_0 and for larger W/λ_0, but one can discern that in the intermediate range the EDC values are very slightly higher than the accurate ones. The agreement is excellent, though, and the use of the EDC method here is certainly recommended.

Such good agreement explains why the theoretical calculations made by Itoh in his original paper [6] on the inverted strip guide, using the EDC method, agreed so well with his measurements even though his structure functions in the leakage range [23].

A recent paper by Mittra *et al.* [24] also presents accurate mode-matching results for β for the inverted strip guide, using 7 TE and 7 TM modes, and compares them at certain specific points with results obtained via the EDC method. They also found excellent agreement between the sets of values. Unfortunately, however, they did not look for complex roots of their determinantal equation, and they therefore computed only β and not α, thereby missing entirely the new physical effects discussed in Section III.

Our third case relates to the integrated optics field and consists of the rib waveguide, shown in the inset in Fig. 11. The geometry permits a TE surface wave to leak when the guided modes are TM-like. The dispersion curves of $(n_{eff})_g$ versus W/λ_0 for the lowest TM-like guided mode, computed using the EDC method (dashed curve) and the mode-matching procedure (solid curve), are shown in Fig. 11. The difference between the approximate and the accurate curves can now be noticed, but the difference is rather

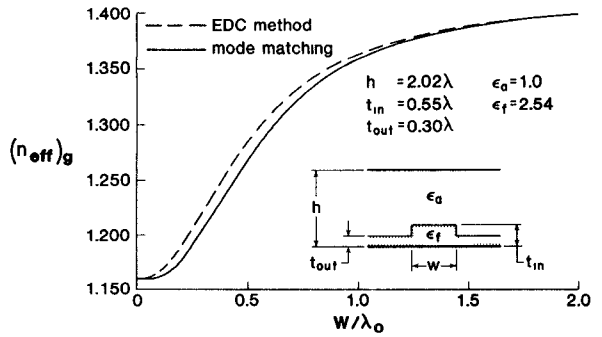

Fig. 12. Dispersion curve for the lowest TE-like guided mode on the dielectric ridge waveguide shown in the inset. (Dimension h in the inset is not drawn to scale.) In this case, the EDC values are noticeably different from those computed from the accurate mode-matching procedure, but the differences are still small.

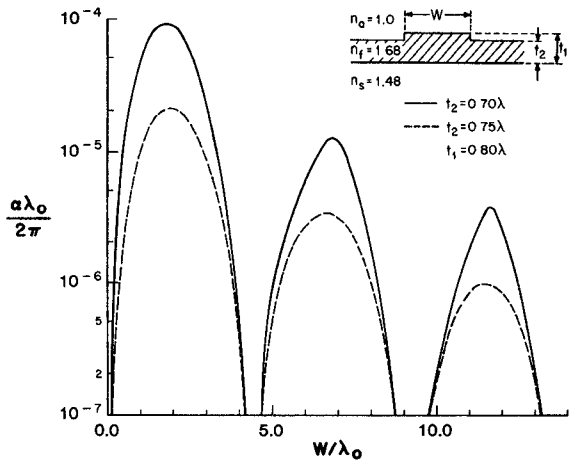

Fig. 13. Curves of attenuation constant α, due to leakage of the TE surface wave, as a function of strip width W for the lowest TM-like guided mode on a rib waveguide for integrated optics, for two different film thicknesses. The numerical values neglect the effect of the continuous spectrum (from reference [25]).

small, and the EDC results are acceptably accurate.

The last of the four cases, applicable to the millimeter-wave field, involves the dielectric ridge waveguide (a variant of the "insular" guide, with the strip and film dielectric materials being the same), shown in the inset in Fig. 12. The guided mode here is TE-like, and a TM surface wave leaks. The curves in Fig. 12 again represent the variation of $(n_{\text{eff}})_g$ with W/λ_0 for the lowest TE-like guided mode. For this case, the difference between the approximate (EDC, dashed line) and accurate (mode-matching, solid line) curves is quite evident. At W/λ_0 near 0.5, for example, the discrepancy between the two curves is about 1.4 percent. This discrepancy may be unimportant for many applications, but its existence should be noted.

From the comparisons presented in Figs. 9 through 12, we may make several observations. The approximate EDC results are of sufficient accuracy for that method to be recommended for the calculation of β for most dielectric waveguide configurations. When are the EDC results less reliable? It is noted that the transverse discontinuities at the sides of the strips in the structures shown in the insets in Figs. 9 through 12 become successively more pronounced. In the inverted strip guides, most of the energy resides in the upper layer, not in the strip, so that the strip sides offer an electrically-small transverse discontinuity. In the rib and ridge guides of Figs. 11 and 12, the strip plays a stronger role, but the step in the rib guide of Fig. 11 is clearly smaller than that in the ridge guide of Fig. 12. It is also true that the amount of leakage in each case is related to the importance of the step discontinuity at the strip sides. We may, therefore, state that the EDC method may be relied upon to produce accurate values for β (or $(n_{\text{eff}})_g$) except when the leakage rate is large or, alternatively, the sides of the strip represent an electrically-important step discontinuity.

B. Examples of Leakage and Resonance Effects

Depending on the type of waveguide and on the specific geometrical parameters, the rate of leakage may be large or small, the exit angle θ_{out} (see Fig. 8) of the surface wave may be large or small, and the leakage may occur for any value of strip width or only for narrow strip widths. The physical bases for these distinctions are discussed in Section III; here we present four specific examples to indicate these features numerically. The examples involve the rib waveguide for integrated optics, where comparison is made with calculations by others, the dielectric ridge waveguide for millimeter waves, which exhibits an enormous leakage rate, and two inverted strip waveguides, one of which leaks a TE surface wave and the other a TM surface wave.

1) Rib Waveguide for Integrated Optics: The first set of leakage calculations discussed here was made for the rib waveguide, shown in Fig. 3(e), and also in the inset on Fig. 13, where specific dimensions and refractive indices are given. Theoretical calculations were first performed taking the TE–TM coupling into account correctly, assuming that only the dominant surface waves of each type can propagate in the constituent inside and outside regions (valid for the film thicknesses chosen), but neglecting the higher modes (or, alternatively, the continuous spectrum, if the structure is truly open). Later, more accurate calculations were made employing the mode-matching procedure discussed in Part I, taking 15 TE modes and 15 TM modes in each constituent region.

The above-mentioned early calculations were published in 1978 [25]. In that paper, dispersion curves in the form of n_{eff} versus W/λ_0, where W is the strip width, were presented for two different film thicknesses, and curves of attenuation due to leakage versus W/λ_0 were also given. The calculations were made for the two lowest TM-like guided modes of the rib waveguide, where the lowest mode is that for which the midplane is a magnetic wall, or open circuit. It was found that the dispersion curves (for n_{eff}) differed very little from those computed by the EDC method, which neglects the TE–TM coupling entirely, as discussed in Section II-A.

The curve of attenuation versus W/λ_0, on the other hand, is very interesting, and is reproduced here as Fig. 13. It should first be recognized that if the TE–TM coupling did not occur there would be no attenuation, since we are

neglecting material losses. Therefore, *all* the attenuation shown is due to *leakage*.

The numerical values for α of the lowest TM-like guided mode are of the order of the measured results, so that the leakage effect is significant, though small. The leakage is seen to be greater for greater rib height, as expected since then a larger step discontinuity occurs at the strip side. The leakage also decreases as the strip width W increases. This occurs because, as W increases, the constituent surface waves inside the strip region approach closer to glancing incidence, and the coupled components decrease in amplitude. For this choice of geometrical parameters, leakage occurs for *all* values of strip width W, so that the curves would continue further as W/λ_0 increased.

In addition, it is evident from Fig. 13 that a *resonance* (or a cancellation) effect is occurring. It is due to the TE surface wave inside, which is bouncing back and forth above cutoff, as explained in Section III-C. For this case, condition (2) for the resonance effect, namely,

$$\left(k_x^{\mathrm{TE}}\right)_{\mathrm{in}} W = 2\pi$$

for the first resonance, is within 1 percent; the second resonance is within 1 percent of 4π, and so on.

Using our earlier work [25] as the starting point, Ogusu *et al.* [26] improved the numerical values by employing a mode-matching procedure similar to the one described in Part I. They used 10 TE and 10 TM modes in their calculations, but they did not directly obtain the complex roots, as we do. Instead, they solved for the real part of the roots, thereby obtaining the values of β, and then they determined the values of α using a clever approximation based on their computed values of β. Their published results indicated that our earlier calculations [25] were too low by nearly an order of magnitude, but those results puzzled us as our later, accurate calculations showed that our early calculations were too large rather than too small. A few months later, however, they published a correction [27]; they had neglected a factor of $(1.6\pi)^2 \cong 25$ in their results. The recomputed values for α then agreed rather well numerically with our own more accurate results, as shown in Fig. 14, except for the region around the resonance or cancellation points. We believe that their inability to achieve deeper cancellations is due to the approximation they used to derive their values of α.

It should be noted that the accuracies achievable by these theoretical calculations are excellent with respect to any engineering needs, particularly since additional contributions to the total attenuation arise due to material losses and to scattering losses due to rough surfaces or material inhomogeneities. The discrepancies at the minima (resonances) appearing in Fig. 14 are important on theoretical grounds, but of lesser importance from a practical standpoint since the values there are at least two orders of magnitude below the value at the maximum. Both theoretical methods for achieving the values of α should, therefore, be viewed as very good ones.

The dispersion curve of $(n_{\mathrm{eff}})_g$ versus W/λ_0 for this structure is presented in Section IV-A in the context of a discussion relating to the accuracy of β (or n_{eff}) calculations made using the EDC method.

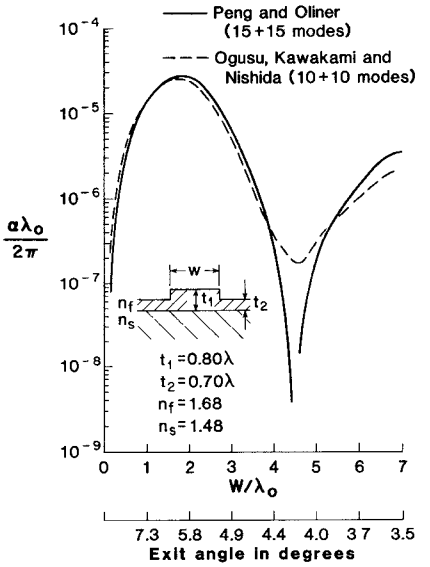

Fig. 14. Leakage values for the rib waveguide of Fig. 13, where the numerical values include the effect of the continuous spectrum and are now accurate, and comparison with corresponding calculations taken from [27]. The comparison is very good except in the vicinity of the sharp resonance dips. Selected values of the leakage exit angle θ_{out} are presented on a second abscissa axis.

An additional quantity of importance is the *leakage angle* θ_{out} (see Fig. 8) of the leaking TE surface wave, which is readily determined using relation (3). Values of θ_{out} for several values of W/λ_0 are included on a second abscissa scale in Fig. 14. It is seen that θ_{out} is about 6.1° at the first maximum in leakage attenuation, and about 3.5° at the second maximum. The variation is in agreement with the general behavior noted in Section III-E, namely, that the angle becomes smaller as the strip width increases. For this optical rib guide, the exit angle θ_{out} of the leakage is relatively small. In fact, we have found from several calculations of the guidance behavior of waveguides for integrated optics that the leakage angle θ_{out} is generally relatively small in the optical context.

2) Dielectric Ridge Waveguide for Millimeter Waves: This second waveguiding structure is selected to illustrate three important differences in leakage performance from that just discussed above for the rib waveguide. In the preceding calculations, we saw that leakage occurs for all values of strip width; here we present a case for which leakage occurs only for narrow strip widths. For the preceding case, the leakage rate was significant, but not large; here, it is spectacularly large. Finally, for the rib waveguide above, the angle of the leaking surface wave was relatively small, whereas here it is quite large.

The plot of attenuation constant as a function of strip width for this dielectric ridge waveguide is presented in Fig. 15. The structure and its geometrical parameter values are shown in the inset on that figure. Let us consider the three features mentioned above.

a) One first notes in Fig. 15 that the attenuation, and therefore the leakage, remains zero for strip widths W

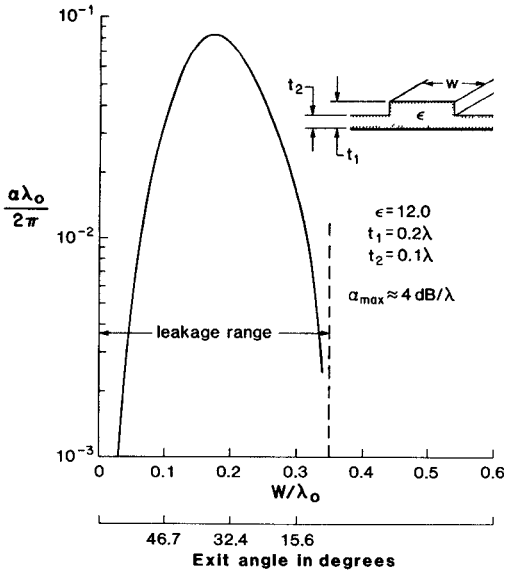

Fig. 15. Curve of attenuation constant α, due to leakage of the TM surface wave, as a function of strip width W for the lowest TE-like guided mode on the dielectric ridge guide shown in the inset. For these parameters, leakage occurs only for narrow strip widths, but the leakage rate is enormous. Selected values of the leakage exit angle are presented on a second abscissa axis.

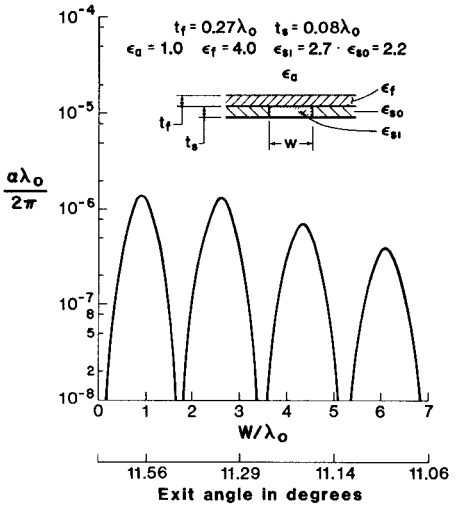

Fig. 16. Attenuation constant α, due to leakage of the TM surface wave, as a function of strip width W for the lowest TE-like guided mode on the inverted strip guide shown in the inset. Leakage occurs for all values of strip width, but the amount is negligibly small. Leakage exit angles are presented on a second abscissa axis.

greater than about 0.35 λ_0. This type of waveguide will not leak for "TM" excitation, resulting in TM-like guided modes which are purely bound, but can leak for "TE" excitation, for which the TE-like guided modes may or may not be leaky, depending on the guide's dimensional parameters. For the choice of dimensions indicated in Fig. 15, the waveguide will leak only when its width is relatively narrow.

b) The maximum value of the attenuation in this case is more than three orders of magnitude greater than that shown in Fig. 14, being as large as 4 dB per wavelength! Several optimizations have been combined deliberately here in order to maximize the leakage achievable in this test example. First of all, the material chosen is silicon, which has a high value of dielectric constant ($\epsilon = 12.0$), to enhance the contrast between the n_{eff} values of the inside and outside regions. The second step taken to enhance that contrast is to make the ratio of t_1/t_2, the strip plus film height to film height, equal to 2:1, rather than about 1.14:1, as in Fig. 14. These two steps serve to produce a severe geometrical and electrical discontinuity at the strip sides, thus greatly increasing the leakage produced. Although such huge values of leakage rate will not usually be achieved in practice, it is important to know that large values are possible. It should also be remembered that one can adjust the leakage rate to be large or small, or zero, depending on the choice of dimensional parameters.

c) The exit angle θ_{out} of the leaking TM surface wave, computed using relation (3), is shown on a second abscissa scale in Fig. 15 for three values of W/λ_0. It is seen that, at the maximum of the leakage, the leakage angle is about 36°, a value much larger than that found in the rib guide for integrated optics. It is also to be noted that θ_{out} approaches zero at the edge of the leakage range.

3) Inverted Strip Waveguide for Millimeter Waves: For the two waveguiding structures discussed in 1 and 2, the hybrid guided modes based on the dominant, or lowest, surface-wave mode in the constituent regions never leak. However, the guided modes based on the surface-wave mode of opposite polarization may leak or not, depending on the geometrical parameters. These features are discussed in more detail in Section III-D.

The inverted strip waveguide (see Fig. 4) is customarily excited in "TM" fashion, resulting in TM-like guided modes. It is generally assumed that such modes are the dominant modes on the structure. According to the rule mentioned above, those modes should not leak. Those modes sometimes do leak, however, as we show below, because for those particular dimensions the "TM" incidence does *not* actually excite the dominant surface wave in the constituent regions. Therefore, the inverted strip guide is an example of a *versatile* waveguiding structure for which we may select either the TM-like or the TE-like guided modes to be leaky, depending on the relative dimensions and dielectric constants. To illustrate this feature, we present now an example of each case.

a) We first consider a structure for which the TE-like guided modes will leak. The curve of $(n_{\text{eff}})_g$ versus W/λ_0 for this structure is presented in Fig. 9 of Section IV-A, as an illustration of a case for which the EDC method of calculating β (or n_{eff}) yields highly accurate results. The inset on that figure shows that the structure has a thick layer and a thin strip, although that is not always required for leaky TE-like guided modes.

The attenuation versus W/λ_0 behavior is indicated in Fig. 16, where it is seen that leakage occurs for all values of strip width. The value of α at the maximum is approximately 6×10^{-5} dB per wavelength, which represents a very small leakage rate for a millimeter-wave application. This negligibly-small leakage rate occurs here because the discontinuity due to the side of the strip is electrically very

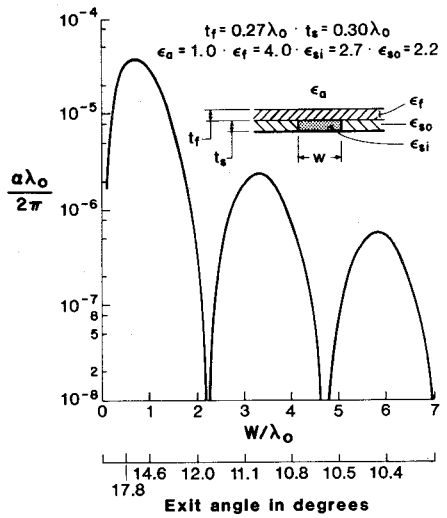

Fig. 17. Attenuation constant α, due to leakage of the TE surface wave, as a function of strip width W for the lowest TM-like guided mode on the inverted strip guide shown in the inset; the waveguide differs from that in Fig. 16 only in the value of t_s but that modification is sufficient to reverse the polarization of the leakage. Leakage occurs for all values of strip width. Leakage exit angles are presented on a second abscissa axis.

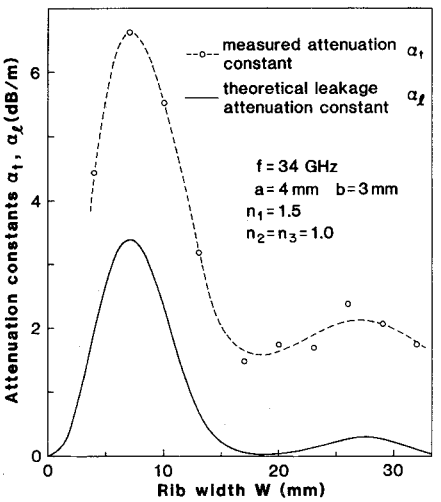

Fig. 18. Measured values of total attenuation for a rib waveguide with no substrate, modeled at millimeter wavelengths, and comparison with theoretical calculations for leakage only. (Note that the ordinate scale is linear rather than logarithmic, as in Figs. 13 to 17.) The (larger) measured values include material and coupling losses, but the close correspondence in curve shapes verifies the theoretical analysis. (From reference [28]).

small, both because the strip is thin compared to the layer above, which carries most of the power, and because the dielectric constant ϵ_{so} (=2.2) placed outside of the central strip region is only slightly different from ϵ_{si} (=2.7) in the strip itself. In the usual inverted strip guide, $\epsilon_{so} = 1.0$, so that the leakage rate is quite a bit larger.

An examination of the values of W corresponding to the resonance dips, which are very pronounced in Fig. 16, verify condition (2) of Section III-C. The agreements were to within 0.5 percent for each of the dips.

The exit angle of the leaking TM surface wave is found to be about 11° in this case. The exit angles θ_{out} for selected values of W/λ_0 are also marked on a second abscissa on the plot in Fig. 16.

b) In this second example, the thickness t_s of the strip is increased substantially and made approximately equal to that of the layer; the dielectric constants and all of the other dimensions remain unchanged. This change in strip thickness is sufficient to *reverse* the dominant polarization, so that now the TM-like guided modes become leaky. The curve of $(n_{\text{eff}})_g$ versus W/λ_0 appears as Fig. 10 of Section IV-A, and the attenuation vs. W/λ_0 behavior is shown in Fig. 17.

One first sees from Fig. 17 that leakage occurs on this structure for all values of strip width. The value of α at the maximum is now approximately 3×10^{-3} dB per wavelength, still small but much larger than that in Fig. 16, and no longer negligible. Since the strip thickness is now greater, the discontinuity at the strip side is more important here; if the ϵ_{so} were also changed to unity, the leakage rate would increase further. The nonunity ϵ_{so} was chosen here to demonstrate in an easy way that a small change (in strip thickness in this case) can produce the perhaps-surprising switch in the polarization of the guided modes which can leak.

The resonance dips are also pronounced here, and condition (2) is again verified very closely, to within less than 0.5 percent for the three nulls shown in Fig. 17. The exit angles θ_{out} of the leaking TE surface wave, which are shown on a second abscissa in Fig. 17 for selected values of W/λ_0, are somewhat larger now; they vary from roughly 17° at the first maximum to 10° at the third maximum.

C. Experimental Confirmation

Very little experimental data are available so far, because the leakage effect is not yet widely known. An experiment by Ogusu and Tanaka [28] was performed recently in Japan, however, in order to verify the existence of the leakage. The experiment was conducted at millimeter wavelengths to improve the accuracy of the measurements.

The structure on which measurements were performed was a rib waveguide for which the substrate was taken to be air. The refractive index of the film and strip was equal to 1.5 (polypropylene), and the values of t_1 and t_2 (see Fig. 13) were 4.0 and 3.0 mm, with the frequency equal to 34.0 GHz. The insertion loss was measured for various lengths of the waveguide, and the attenuation was obtained from a plot of insertion loss versus length. Such measurements were made over a wide range of strip widths W.

Calculations of the leakage as a function of W were also made by Ogusu and Tanaka using the method of [26]. A comparison between these theoretical values and the measured values [28] are shown in Fig. 18. (Let us note that the ordinate axis for these plots employs a linear scale rather than the logarithmic one used in Figs. 13–17.) It is seen that the two curves are very similar in shape, with maxima and minima in α occurring at the same values of W. The curve representing the measured values is substantially higher than the theoretical curve because the measurements also include the material losses and losses occurring at the

feed end and the termination of the waveguiding structure being measured. The close correlation between the measured and calculated curves shows clearly that the principal characteristics of the leakage produced are correctly described by the theoretical analysis.

REFERENCES

[1] E. W. Hu, S. T. Peng, and A. A. Oliner, "A novel leaky-wave strip waveguide directional coupler," in *Topical Meet. Integrated and Guided Wave Optics*, Paper No. WD2 (Salt Lake City, UT), Jan. 1978.

[2] R. M. Knox and P. P. Toulios, "Integrated circuits for the millimeter wave through optical frequency range," in *Proc. Symp. Submillimeter Waves*, Brooklyn, NY: Polytechnic Press, Apr. 1970, pp. 497–516.

[3] A. A. Oliner, R. C. M. Li, and H. L. Bertoni, "Microwave network approach to guided acoustic surface wave structures," Final Rep. ECOM-0418-F, Polytechnic Inst. Brooklyn, Brooklyn, NY, Rep. PIBEP-71-092, Aug. 1971.

[4] A. A. Oliner, "Microwave methods for acoustic surface waves and waveguides," presented at 1971 Int. Symposium on Antennas and Propagation, Sendai, Japan, Sept. 1971.

[5] W. V. McLevige, T. Itoh, and R. Mittra, "New waveguide structures for millimeter-wave and optical integrated circuits," *IEEE Trans. Microwave Theory Tech.*, vol. MTT-23, pp. 788–794, Oct. 1975.

[6] T. Itoh, "Inverted strip dielectric waveguide for millimeter-wave integrated circuits," *IEEE Trans. Microwave Theory Tech.*, vol. MTT-24, pp. 821–827, Nov. 1976.

[7] S. Shindo and T. Itanami, "Low-loss rectangular dielectric image line for millimeter-wave integrated circuits," *IEEE Trans. Microwave Theory Tech.*, vol. MTT-26, pp. 747–751, Oct. 1978.

[8] T. E. Rozzi and T. Itoh, "Two dimensional analysis of the GaAs double hetero stripe-geometry laser," in *Proc. European Microwave Conf.*, pp. 495–498 (Rome, Italy), Sept. 1976.

[9] H. Furuta, H. Noda, and A. Ihaya, "Novel optical waveguide for integrated optics," *Appl. Opt.*, vol. 13, pp. 322–326, Feb. 1974.

[10] N. Uchida, "Optical waveguide loaded with high refractive-index strip film," *Appl. Opt.*, vol. 15, pp. 179–182, Jan. 1976.

[11] E. A. J. Marcatili, "Dielectric rectangular waveguide and directional coupler for integrated optics," *Bell Syst. Tech. J.*, vol. 48, pp. 2071–2102, Sept. 1969.

[12] R. M. Knox and P. P. Toulios, "A V-band receiver using image line integrated circuits," in *Proc. National Electronics Conf.*, (Chicago, IL). Oct. 1974.

[13] J. E. Goell, "Rib waveguides for integrated optical circuits," *Appl. Opt.*, vol. 12, pp. 2797–2798, Dec. 1973.

[14] F. K. Reinhart, R. A. Logan, and T. P. Lee, "Transmission properties of rib waveguides formed by anodization of epitaxial GaAs on Al_xGa_{1-x} As layers," *Appl. Phys. Lett.*, vol. 24. pp. 270–272, Mar. 15, 1974.

[15] R. T. Kersten and H. Boroffka, "Ion implantation into fused quartz for integrated optical circuits," *Optics Commun.*, vol. 17, pp. 119–123, Apr. 1976.

[16] R. T. Kersten, "A directional coupler with large waveguide separation," *Optics Commun.*, vol. 17, pp. 124–128, Apr. 1976.

[17] A. A. Oliner, "Optical and acoustical microelectronics: Similarities and differences," in *Proc. Symp. Optical and Acoustical Micro-Electronics* (Polytechnic Inst. of New York), pp. 1–17 (especially 12, 13), Apr. 1974.

[18] J. Hamasaki and K. Nosu, "A partially metal-clad-dielectric-slab waveguide for integrated optics," *IEEE J. Quantum Electron.*, vol. 10, pp. 822–825, Oct. 1974.

[19] Y. Yamamoto, T. Kamiya, and H. Yanai, "Propagation characteristics of a partially metal-clad optical guide: Metal-clad optical strip line," *Appl. Opt.*, vol. 14, pp. 322–326, Feb. 1975.

[20] A. A. Oliner and S. T. Peng, "Waveguides for integrated optics formed by metal platings," in *Proc. 6th European Microwave Conf.*, pp. 499–503 (Rome, Italy), Sept. 1976.

[21] A. A. Oliner and S. T. Peng, "Effects of metal overlays on 3-D optical waveguides," *Appl. Opt.*, vol. 17, no. 18, pp. 2866–2867, Sept. 15, 1978.

[22] ——, "A simple method for predicting when modes will leak on dielectric strip waveguides," to be published.

[23] A. A. Oliner, S. T. Peng, and J. P. Hsu, "New propagation effects for the inverted strip dielectric waveguide for millimeter waves," in *Int. Microwave Symp. Dig.* (Ottawa, Ont., Canada), pp. 408–410, June 1978.

[24] R. Mittra, Y. L. Hou, and V. Jamnejad, "Analysis of open dielectric waveguides using mode-matching technique and variational methods," *IEEE Trans. Microwave Theory Tech.*, vol. MTT-28, pp. 36–43, Jan. 1980.

[25] S. T. Peng and A. A. Oliner, "Leakage and resonance effects on strip waveguides for integrated optics," *Trans. Inst. of Electronics and Commun. Eng. Jap.* (Special Issue on Integrated Optics and Optical Fiber Communications), vol. E61, pp. 151–154, Mar. 1978.

[26] K. Ogusu, S. Kawakami, and S. Nishida, "Optical strip waveguide: An analysis," *Appl. Opt.*, vol. 18, pp. 908–914, Mar. 15, 1979.

[27] *Ibid.*, Correction, vol. 18, p. 3725, Nov. 1979.

[28] K. Ogusu and I. Tanaka, "Optical strip waveguide: An experiment," *Appl. Opt.*, vol. 19, pp. 3322–3325, Oct. 1, 1980.

Arthur A. Oliner (M'47–SM'52–F'61), for a photograph and biography please see page 854 of this issue.

Song-Tsuen Peng (M'74), for a photograph and biography please see page 854 of this issue.

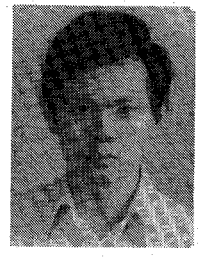

Ting-Ih Hsu (S'78) was born in Taiwan, China, on November 13, 1950. He received the B.S. degree in electrophysics from the National Chiao-Tung University, Taiwan, China, in 1973, and the M.S. degree in electrical engineering from the Polytechnic Institute of New York, Brooklyn, NY, in 1977.

From 1973 to 1975, he served in the Taiwan Military Integrated Communication Agency. From 1975 to 1976, he was an Engineer at General Instrument Microelectronics, Taiwan, where he worked on integrated-circuit chip test equipment design. From 1977 to 1980 he was employed as a Research Fellow at the Polytechnic Institute of New York, where he was involved in research concerned with the propagation and guidance of surface waves. He is currently a development engineer at the Microwave Semiconductor Corporation, Somerset, NJ, where he is working on broadband GaAs FET power amplifier design and development.

Alberto Sanchez received the Licenciatura in physics in June 1970, from the University of Zaragoza, Spain, and the M.S. degree in electrophysics from the Polytechnic Institute of New York, Brooklyn, NY, in June 1978.

He has been a Research Assistant in the Microwave Research Institute of the Polytechnic Institute of New York since 1977. He is a recipient of the Fundación Juan March Scholarship for advanced studies abroad. His research interests lie in the areas of microwave networks, integrated optics and electrooptics.